SPE
Society of Petroleum Engineers

SPE 18418

The Formulation of a Thermal Simulation Model in a Vectorized, General Purpose Reservoir Simulator

by M.C.H. Chien,* H.E. Yardumian, E.Y. Chung, and W.W. Todd,* Chevron Oil Field Research Co.

*SPE Members

This paper was prepared for presentation at the SPE Symposium on Reservoir Simulation in Houston, TX, February 6-8, 1989.

This paper was selected for presentation by an SPE Program Committee following review of information contained in an abstract submitted by the author(s). Contents of the paper, as presented, have not been reviewed by the Society of Petroleum Engineers and are subject to correction by the author(s). The material, as presented, does not necessarily reflect any position of the Society of Petroleum Engineers, its officers, or members. Papers presented at SPE meetings are subject to publication review by Editorial Committees of the Society of Petroleum Engineers. Permission to copy is restricted to an abstract of not more than 300 words. Illustrations may not be copied. The abstract should contain conspicuous acknowledgment of where and by whom the paper is presented. Write Publications Manager, SPE, P.O. Box 833836, Richardson, TX 75083-3836. Telex, 730989 SPEDAL.

ABSTRACT

This paper describes the formulation of a thermal simulation model in a vectorized, general purpose reservoir simulator. The thermal simulation model, an option in this general purpose simulator, is equivalent to a three-phase, three-dimensional, thermal compositional simulator. It has a variety of options for modeling fluid properties and phase behavior. These include the EOS method (the three parameter Peng-Robinson equation of state) and the non-EOS methods (table look-ups and correlations). The model also considers the solubility of water in the oil phase. Furthermore, all calculations are extensively vectorized.

Test problems including problem No. 3 of the Fourth SPE Comparative Solution Project are used to evaluate the effectiveness of vectorization. Results show that the vectorized calculations outperform the nonvectorized ones by about an order of magnitude in computational speed on the Cray X-MP/48. Overall, this thermal model runs about 5 times faster than a previously reported conventional, partially vectorized thermal simulator.

Finally, the use of this thermal simulation option to study the sensitivity of simulation results to various fluid property and phase behavior calculation methods is illustrated with a hypothetical problem. Results show that simulation results can be used to determine the importance of different K-value and volume calculation methods, and the inclusion of water-in-oil solubility.

References and illustrations at end of paper.

INTRODUCTION

In recent years there has been an increasing interest in the development of general purpose reservoir simulators. A general purpose simulator offers easier maintainability by eliminating the need to duplicate routines which are common to many simulators. It also improves the consistency in the simulation results of various recovery processes for the same reservoir. In addition, vectorization can be used to improve the computational speed of such a general purpose simulator so that it becomes feasible to do large scale simulations.

In a previous paper[1], we have described the formulation of a black oil and a compositional option in a vectorized, general purpose reservoir simulator. It was shown that for some models, such a simulator could be an order of magnitude faster than a nonvectorized one.

In this work, we extend the simulator to thermal applications with the objectives of higher computational speed and more accurate modeling of the thermal processes. The high computational speed in the thermal option is obtained by vectorization. The thermal process is modeled more accurately by adding two new features that are not generally found in conventional thermal simulators. First, we have implemented an equation of state option for modeling fluid properties and phase behavior of hydrocarbon phases. An equation of state accounts for the compositional effects on K-value, therefore, it is a more rigorous approach for light oil steam floods. Secondly, we have included an option for water solubility in oil, which can be significant at high temperatures for some light oils.

This paper is divided into several sections. The first section describes the mathematical formulation used in the

simulator. The second section discusses the numerical techniques used to solve the equations. The third section shows how vectorization is applied to achieve efficient calculations. The fourth section evaluates the effectiveness of vectorization and compares its performance with that of a conventional thermal simulator. The fifth section illustrates the sensitivity of the simulation results to various fluid property and phase behavior calculation methods using a hypothetical problem. Finally, the results of this work are summarized.

MATHEMATICAL FORMULATION

The thermal simulation option described here is equivalent to a multicomponent, three-phase, three-dimensional, thermal compositional simulator. It utilizes the fully implicit formulation in order to stabilize the numerical solution. It has various calculation methods for fluid properties and phase behavior. These include the three parameter Peng-Robinson equation of state[2], table look-ups, and correlations. (See Appendix A for available options.) In addition, it can account for the solubility of water in oil. Darcy's law and instantaneous phase equilibrium are assumed to be valid.

Given the above assumptions, we can write the necessary equations for the simulation model. Basically, these equations can be derived from those given in Reference 1. However, we give a detailed description here because of the special treatment of the water component.

Balance Equations

The material balance equations for the hydrocarbon components can be written as

$$\frac{V}{\Delta t}[(\phi z_i)^{n+1} - (\phi z_i)^n]$$

$$-\sum_{j=1}^{N_h}\delta\{T_g(\frac{x_{ij}k_{rj}}{v_j\mu_j})^{n+1}[\delta(p_o^{n+1}+p_{jo}^{n+1})+\rho_j^{n+1}\delta D]\}-q_i=0$$

$$i=1,N_c-\chi \qquad (1)$$

with

$$z_i=\sum_{j=1}^{N_h}\frac{S_j x_{ij}}{v_j} \qquad i=1,N_c-\chi \qquad (2)$$

where χ is a flag for the solubility of water in oil. χ is equal to 1 when water is soluble in the oil phase, otherwise, it is equal to 0. N_h is the number of hydrocarbon phases. Since we are interested in a system with oil and gas, N_h is equal to 2. N_c is the total number of components soluble in the oil phase. Thus, $N_c-\chi$ is the number of hydrocarbon components. x_{ij} is the composition of component i in phase j. In equations (1) - (2), we have used i=1 to $N_c-\chi$ to stand for hydrocarbon components and i=N_c+1-χ to stand for the water component. For convenience of discussion, we will use $\varpi = N_c$+1-χ to stand for the water component. We will also use j=1 to stand for the oil phase, j=2 for the gas phase, and j=3 or j=w for the water phase.

The material balance equation for the water component is written as

$$\frac{V}{\Delta t}[(\phi\frac{S_w}{v_w})^{n+1}-(\phi\frac{S_w}{v_w})^n]$$

$$-\delta[T_g(\frac{k_{rw}}{v_w\mu_w})^{n+1}(\delta(p_o^{n+1}+p_{wo}^{n+1})+\rho_w^{n+1}\delta D)]-q_w=0$$

$$if\ \chi=0 \qquad (3)$$

or

$$\frac{V}{\Delta t}[(\phi z_\varpi)^{n+1}-(\phi z_\varpi)^n]$$

$$-\sum_{j=1}^{N_h}\delta\{T_g(\frac{x_{\varpi j}k_{rj}}{v_j\mu_j})^{n+1}[\delta(p_o^{n+1}+p_{jo}^{n+1})+\rho_j^{n+1}\delta D]\}$$

$$-\delta[T_g(\frac{k_{rw}}{v_w\mu_w})^{n+1}(\delta(p_o^{n+1}+p_{wo}^{n+1})+\rho_w^{n+1}\delta D)]-q_w=0$$

$$if\ \chi=1 \qquad (4)$$

with

$$z_\varpi=\sum_{j=1}^{N_h}\frac{S_j x_{\varpi j}}{v_j}+\frac{S_w}{v_w} \qquad (5)$$

Finally, the energy balance equation is expressed as

$$\frac{V}{\Delta t}[(\phi\sum_{j=1}^{N_h+1}\frac{S_j u_j}{v_j})^{n+1}-(\phi\sum_{j=1}^{N_h+1}\frac{S_j u_j}{v_j})^n$$

$$+(1-\phi)C_p(T^{n+1}-T^n)]$$

$$-\sum_{j=1}^{N_h+1}\delta\{T_g(\frac{h_j k_{rj}}{\mu_j})^{n+1}[\delta(p_o^{n+1}+p_{jo}^{n+1})+\rho_j^{n+1}\delta D]\}$$

$$-\delta(T_h\delta T)-q_h=0 \qquad (6)$$

where j=N_h+1 stands for the water phase.

A key factor that affects the stability of the simulation is the calculation of phase density, ρ_j. This term is needed for the gravity driving force between two cells, $\rho_j\delta D$. In this work, we always use the average density of the two cells to ensure the stability of the simulator. If a phase is

missing from one of the two cells, its density is estimated from stability analysis[3].

Fugacity Equalities for Oil and Gas Phases

When an equation of state is used for phase behavior calculations, the following fugacity equalities can be written for the components that are soluble in the oil and gas phases:

$$f_{ij} = f_{i1} \qquad j = 2, N_h \quad and \quad i = 1, N_c \tag{7}$$

The above equations include the water component if $\chi = 1$.

When a K-value table, instead of an equation of state, is used to calculate phase equilibrium, equation (7) can be interpreted as:

$$\frac{x_{ij}}{K_{ij}} = x_{i1} \quad j = 2, N_h \quad and \quad i = 1, N_c \tag{8}$$

Fugacity Equalities for Water and Oil/Gas Phases

In a thermal simulation, water could exist in the gas phase. Water could also exist in the oil phase if water-in-oil solubility is allowed. Therefore, an additional equation has to be written for the equilibrium of the water component in the water phase and in one of the hydrocarbon phases.

Water Soluble in Oil

If an equation of state is used, the mole fraction of water in one of the hydrocarbon phases can be obtained from

$$f_{we} = p_s \tag{9}$$

f_{we} is the fugacity of the water component in an existing hydrocarbon phase e. Subscript e is 1 when oil exists and 2 when gas exists and oil does not exist. p_s is the saturation pressure of the water phase at the system temperature. Equation (9) assumes that the water phase is an ideal solution, a good approximation for most water-oil mixtures. It becomes a crude approximation only when oil contains highly polar components such as alcohols and ketones.

If a K-value table is used, one of the following equations has to be used:

$$x_{w2} p = p_s \quad \text{if gas exists} \tag{10}$$

$$K_{w2} x_{w1} p = p_s \quad \text{if gas does not exist} \tag{11}$$

In the above equations, we have assumed that the water component in the gas phase behaves like an ideal gas. This assumption is not necessary when an equation of state is used.

Water Not Soluble in Oil

When the water component can only exist in the gas phase but not in the oil phase, that is, when χ=0, the steam mole fraction y_w can be calculated according to

$$y_w = p_s/p \quad \text{if gas exists} \tag{12}$$

Note that when χ=0, y_w instead of x_{w2} is used to stand for the steam mole fraction.

Other Equations

The volume equations are

$$f(p, T, x_{ij}, v_j) = 0 \quad j = 1, N_h \tag{13}$$

When the Peng-Robinson equation of state is used to calculate volume, the above equations reduce to

$$\frac{pv_j}{RT} - \frac{v_j}{v_j - b_j} + \frac{a_j v_j}{v_j(v_j + b_j) + b_j(v_j - b_j)} = 0 \qquad j = 1, N_h \tag{14}$$

The saturation constraint is

$$\sum_{j=1}^{N_h+1} S_j - 1 = 0 \tag{15}$$

The composition constraints are

$$\sum_{i=1}^{N_c} x_{ij} = 1 \quad j = 1, N_h \quad if\ \chi = 1$$

$$\sum_{i=1}^{N_c} x_{ij} + \delta_{2j} y_w = 1 \quad j = 1, N_h \quad if\ \chi = 0 \tag{16}$$

In the above equations, the number of unknowns to be solved is the same as the number of equations. This is summarized in Table 1 where we have ordered the unknowns and the equations for the purpose of illustration. This order has no implication on the selection of primary variables. The selection is discussed in the next section. Equations (1) - (16) are written for each grid block, therefore, each grid block has its own set of equations and unknowns.

NUMERICAL SOLUTION PROCEDURES

The numerical procedures for solving equations (1) - (16) have been described in a previous paper[1]. Here, we only outline the procedures that are important for a thermal simulator.

Perhaps the most important step in the numerical solution procedures is the selection of the primary variables. The primary variables are those that remain after variable reduction using the constraint equations. They are solved from the material and energy balance equations. These variables have to be independent, otherwise, the Jacobian matrix becomes singular. In this work, they are selected according to the fluid type in a grid block.

The selection of primary variables is outlined in Table 2. When gas and water coexist in a grid block, the selection also depends on the boiling point range of the gas-water mixture. The boiling point range is the range of temperatures exhibited by a fluid when it is evaporated at constant pressure. Figure 1 shows two typical boiling point ranges: narrow and wide, observed in a laboratory. A narrow range implies that temperature and pressure are not independent of each other, i.e. one can be inferred from the other. Therefore, only one of them can be the primary variable. Here, we select pressure as the primary variable. A wide range implies that temperature and pressure are fairly independent, and it is less likely to infer one from the other. Therefore, both pressure and temperature have to be in the primary variable list.

The narrow boiling point range is observed in a geothermal reservoir or in a reservoir with dead oil, and a wide boiling point range is observed in a reservoir with light oil. This is consistent with the Gibbs phase rule, which stipulates that for n components in p phases there are f = n-p+2 degrees of freedom. The fluids in a geothermal or dead oil reservoir can be considered pure water systems as far as the phase rule for the gas-water mixture is concerned. The rule then says that there is only one degree of freedom when water and vapor coexist in the reservoir, because n=1, p=2, and f=1. Therefore, only temperature or pressure can be varied independently, but not both. For a light oil reservoir, many oil components can also exist in the vapor phase, making $n \geq 2$ and $f \geq 2$ in the phase rule. Therefore, both temperature and pressure are independent.

During a simulation, a grid block could switch from a wide boiling point range to a narrow boiling point range. This occurs when all vaporizable oil components are essentially depleted from the grid block. The way we determine the boiling point range is to check the non-steam mole fraction. A low non-steam mole fraction in a grid block implies a narrow boiling point range.

VECTORIZATION

As described in a previous paper[1], efficient vectorization requires a long vector length. One way to obtain a long vector length in reservoir simulation is to construct the vectors by grouping the grid blocks of a given fluid type.

In this work, the cells are divided into 5 types as shown in Table 2. We do not further divide the gas-oil-water type or the gas-water type into two subgroups according to their boiling point ranges. The calculations of the same fluid type but of different boiling point ranges differ only in the selection of primary variables, which is only a small portion of the calculations. For that portion, vectorization can still be achieved by using an IF test within a vector loop to distinguish different boiling point ranges. Details on grouping the cells and vectorizing the calculations can be found in Reference 1.

EVALUATION OF PERFORMANCE

Description of Tests

In this section, we examine the performance of the thermal simulation model based on several test runs on the Cray X-MP/48. We will study the efficiency of vectorization, and compare the speed of the thermal model with that of a conventional thermal simulator.

The model (model A) used to test the efficiency of vectorization is a steam displacement of a distillable oil. The reservoir was discretized into an 18x18x4 grid, and contained oil with 3 components. The fluid and rock characterizations were taken from problem No. 3 of the Fourth SPE Comparative Solution Project[4]. A complete description of the model can be found in Appendix B.

The models used to compare the speed of the thermal simulation option with that of a conventional thermal simulator are model A and problem No. 3 of the Fourth SPE Comparative Solution Project (Model B). The conventional thermal simulator used for this paper is the same one used for the Fourth SPE Comparative Solution Project [4], but with partial vectorization and some enhancements added.

The standard 7 point method was used in all test runs. We made no attempt to reduce grid orientation effects by using an 11 point method.

Efficiency of Vectorization

To study the efficiency of vectorization, we made runs with vectorization turned on and off. The vector-off run was a run using object code compiled on the Cray with the vector processing capability turned off. For the vector-on runs, we also varied the vector length to study the efficiency of vectorization as a function of vector length. The variation was accomplished by specifying a maximum vector length, NVR, in the inner loop.

Table 3 reports the computation time speedups of vector mode runs with different vector lenghts, over scalar mode runs. The routines used include PHYSIC which calculates physical properties, FLOW which calculates flow terms, and SOURCE which performs well related calculations.

The speedup due to vectorization, which is defined as the CPU time of the scalar mode divided by that of the vector mode, varies substantially. The speedup of FLOW is better than that of PHYSIC because the flow calculations were executed with a vector length equal to NVR, whereas in the latter calculations, the actual vector length is limited not only by NVR but also by the number of grid blocks of a given fluid type. For both calculations, the speedup increases with NVR. This is also shown in Figure 2. FLOW reaches a maximum speedup of 9 and PHYSIC reaches a maximum speedup of 8. Routine SOURCE does not take advantage of vectorization. Although the linear equation solution is already vectorized, it is still the most expensive calculation of all, using about 60% of the overall CPU time.

Comparison With a Conventional Thermal Simulator

Table 4 reports the overall CPU time speedups for two models using the thermal option of the vectorized, general purpose simulator and a conventional thermal simulator (C). The table shows that the general purpose simulator is about 5 times faster than simulator C. This speedup is attributed to vectorization as well as a lower number of iterations.

SENSITIVITY OF SIMULATION RESULTS TO FLUID PROPERTY CALCULATION METHODS

The thermal model in the general purpose reservoir simulator has various calculation methods for fluid properties and phase behavior. These methods can be classified into two categories: the EOS (equation of state) method and the non-EOS methods (see Appendix A). The three paramenter Peng-Robinson equation of state is used for the EOS method. The non-EOS methods neglect compositional effects on the K-values and assume no excess heat or volume during mixing. In addition, component fluid properties are represented by tables or simplified functions. These assumptions or simplifications are adequate for heavy oil steam floods, but may introduce errors for light oil steam floods or other nonconventional thermal processes. The EOS method assumes no such simplifications and is a more rigorous approach for all thermal processes.

In this section, we use a hypothetical model to illustrate how the thermal option of the general purpose simulator can be used to study the sensitivity of simulation results to various fluid property calculation methods.

We first used the equation of state for all fluid properties and phase behavior calculations to simulate the process. We called this the reference case. Then, we conducted simulations by replacing the equation of state with a non-EOS method for a selected fluid property (K-value, volume, or enthalpy). Results were compared with the reference case and the errors caused by the non-EOS methods were investigated.

Description Of Test Models

A light oil steam flood was used to test the sensitivity of the simulation results to different physical property calculation methods. Necessary information for the model is shown in Appendix C.

The equation of state parameters are given in Table 5. The third parameter, S_c, for the water component is obtained by fitting water densities at 174° F. Parameters for non-EOS methods are given in Tables 6 and 7. In Table 6, the densities at a standard condition for methane and ethane are estimated from the partial molar volumes via the Standing correlation[5]. The component gas compressibility tables, which are necessary for a non-EOS method, are not reported in this paper. They can be generated from the Peng-Robinson Equation of state using parameters given in Table 5.

Comparison Of Simulation Results

Figures 3 to 8 compare the results for Model C. For this hypothetical problem, using table look-up instead of the equation of state for K-values seems to introduce the least errors in simulation results. This is generally not true for a miscible flood where due to the exchange of components between gas and oil, K-values are strong functions of compositions. The lack of compositional dependency in K-values for Model C reflects little exchange of components between steam and oil.

Replacing the equation of state with correlations for the enthalpy calculations results in slightly lower average reservoir temperatures, but still gives similar oil recovery responses. A lower average reservoir temperature is observed when a gas cap is formed in the primary depletion period. This is because the correlations overpredict the heat of vaporization. Using separate functions for the oil and gas enthalpies, the correlations become inaccurate when the critical point region is approached. This is because in this region the oil and gas enthalpies should approach each other, which can only be reproduced by using the same functions for both the oil and gas enthalpies.

Simulation results for this hypothetical problem are most sensitive to the volume calculation methods. The non-EOS methods, which neglect excess volume of mixing, give higher oil production in the early period, although the final oil recovery approaches that of the EOS method. The use of ideal gas for gas volume results in even higher oil production in the early period. At one point, it is almost 20% higher than the reference case. In both cases, the higher oil production results from the higher pressure support which

is due to larger phase volumes predicted by the non-EOS methods.

It was also found that using an equation of state for fluid property calculations can double the CPU time in the Jacobian generation. This does not drastically inflate the overall CPU time because for large thermal studies, most of the CPU time is spent in the linear equation solution.

CONCLUSIONS

A thermal simulation model has been developed in a general purpose reservoir simulator. The model can account for compositional effects through the use of an equation of state. In addition, it includes the water-in-oil solubility effect. The simulator is extensively vectorized for the Cray. The following summarize the performance of the simulator.

1. An order of magnitude speedup can be achieved with vectorization.
2. Although the linear equation solution is vectorized, it still includes the most expensive calculations of all, particularly for large models with multiple components.
3. The thermal option of the general purpose reservoir simulator is about 5 times faster than a conventional thermal simulator.
4. The thermal option of the simulator can be used to determine the importance of different K-value and volume calculation methods, and the inclusion of water-in-oil solubility.

NOMENCLATURE

a	Attractive force parameter in the Peng-Robinson equation of state
b	Volume parameter in the Peng-Robinson equation of state
c	Fluid compressibility
C_p	Rock heat capacity
C_{pio}	Oil heat capacity for component i
C_{pig}	Gas heat capacity coefficient for component i
D	Depth
f	Fugacity
h	Enthalpy
H_v	Heat of vaporization
k_r	Relative Permeability
K	K-value (Phase Equilibrium Ratio)
M_w	Molecular weight
N_c	Number of Hydrocarbon Components
N_h	Number of Hydrocarbon Phases
p	Pressure
p_{jo}	Capillary pressure of phase j referencing to oil phase (i.e. $p_j - p_o$)
q	Production or injection rate
R	Gas constant
S	Saturation
T	Temperature
T_b	Boiling point temperature
T_g	Geometric part of fluid flow transmissibility
T_h	Heat conduction transmissibility
t	Time or thermal expansion coefficient
u	Internal energy
V	Pore volume
v	Molar volume
x	Phase composition or Oil Phase Composition
y	Vapor Phase composition
Z	Gas compressibility factor
z	Overall concentration

Greek Letters

Δ	Difference operator in time
δ	Difference operator in space or Kronecker delta
μ	Viscosity
ρ	Density
ϕ	Porosity
χ	Flag for Water Solubility in Oil

Superscripts

$m, n, n+1$	Time step levels
s	Saturation pressure or temperature
0	Standard pressure or temperature
1	Reference state for enthalpy calculation

Subscripts

c	Critical condition
e	Existing hydrocarbon phase
i	Component i
j	Phase j
o	Oil phase
w	Water phase
ϖ	Water component

REFERENCES

1) Chien, M. C. H., M. L. Wasserman, H. E. Yardumian, E. Y. Chung, T. Nguyen, and J. Larson: "The Use of Vectorization and Parallel Processing for Reservoir Simulation", paper SPE 16025 presented at the ninth SPE Reservoir Simulation Symposium held in San Antonio, TX, February 1-4,1987.

2) Chien, M. C. H. and M. R. Monroy: "Two New Density Correlations", paper SPE 15676 presented at the 61st Annual Technical Conference and Exhibition of the SPE held in New Orleans, LA, October 5-8, 1986.

3) Michelsen, M. L., "The Isothermal Flash Problem. I. Stability", Fluid Phase Equilibria, 9, 1(1982).

4) Aziz, K. and P. T. Woo: " Fourth SPE Comparative Solution Project: A Comparison of Steam Injection Simulators", paper SPE 13510 presented at the eighth SPE Reservoir Simulation Symposium held in Dallas, TX, February 10-13,1985.

5) Standing, M. B. and Katz, D. L.: "Density of Crude Oils Saturated with Natural Gas", Trans. AIME (1942) 146, 159-165.

6) Steam Tables, Combustion Engineering, Inc., Windsor, Conn. (1967).

7a) MaCleod, D. B.: "On a Relation Between Surface Tension and Density", Trans. Faraday Soc., (1923) Vol. 19, 38-43.

7b) Sudgen, S.: "The Variation of Surface Tension with Temperature and Some Related Fuctions", J. Chem. Soc., (1924) 32-41.

8) Lohrenz, J., Bray, B. G., and Clark, C. R.: "Calculating Viscosity of Reservoir Fluids From Their Composition", J. Pet. Tech. (Oct. 1964) 1171-1176; Trans., AIME, 231.

9) Lee, A. L., Gonzales, M. H., and Eakin, B., E.: "The Viscosity of Natural Gases", J. Pet. Tech. (Aug. 1966) 997.

10) J. E. Killough and C. A. Kossack: " Fifth Comparative Solution Project: Evaluation of Miscible Flood Simulators", paper SPE 16000 presented at the ninth SPE Reservoir Simulation Symposium held in San Antonio, TX, February 1-4,1987.

APPENDIX A : FLUID PROPERTY CALCULATION METHODS

This Appendix describes the fluid property calculation methods available in the thermal model of the general purpose reservoir simulator. We first describe the water phase property calculation methods and then the oil-gas phase property calculation methods. Discussions of the oil-gas phase fluid properties include K-value, volume, viscosity, interfacial tension, enthalpy, and internal energy calculations.

Water Phase Properties

Water density, viscosity, and enthalpy are required for thermal simulations. This simulator first uses steam tables[6] to obtain the saturated properties. Density and enthalpy are then calculated from these saturated properties as follows:

$$\rho_w = \rho_w^s(1 + c_w(p - p^s)) \qquad (A-1)$$

$$h_w = u_w = u_w^s \qquad (A-2)$$

where the superscript s denotes the water properties at temperature T and the corresponding saturation pressure p^s. Note that a correction is necessary to get the water density at T and p from that at T and p^s, while no correction is necessary for the water enthalpy and internal energy if it is assumed that pressure effects are negligible. The water viscosity is given by

$$\ln \mu_w = \ln \mu_w^1 (\frac{1}{T} - \frac{1}{T^1}) \qquad (A-3)$$

where μ_w^1 is the water viscosity at reference temperature T^1.

Oil – Gas Phase Properties

While the water component exists in the gas phase for thermal simulations, it may not exist in the oil phase. When water is soluble in oil, the N_c components include the water component, that is, $N_c - \chi$ is the actual number of hydrocarbon components.

K – value

K-values can be calculated from K-value tables or the three parameter Peng-Robinson equation of state[2](PR3). The number of components that require K-value calculations is N_c. This means that K-values or equation of state parameters for the water component are also required when $\chi = 1$.

In the K-value table option, K-values are functions of pressure and temperature.

Volume

Two options are available for oil and gas phase volume calculations: the three parameter Peng-Robinson equation of state(PR3) and the ideal mixing rule of component volumes.

With the PR3 method, the simulator first calculates v_{nj}, the partial molar volume of the N_c components, by solving equation (14). v_{nj} is the phase volume if the N_c components include all the components in that phase. However, if the N_c components do not include the water component, which is the case when χ =0, the phase volume is obtained by molarly averaging the partial molar volumes of the N_c components and the partial molar volume of the water component as follows:

$$v_j = x_{nj}v_{nj} + (1-\chi)x_{wj}v_{wj} \qquad (A-4)$$

x_{wj} is the composition of the water component in phase j: the steam mole fraction when j is the gas phase, the water solubility in oil when j is the oil phase. Obviously, x_{wo} is zero when $\chi = 0$. The overall composition of the N_c components in phase j, x_{nj}, is given by

$$x_{nj} = \sum_{i=1}^{N_c} x_{ij} \qquad (A-5)$$

The v_{wj} is calculated as follows:

$$v_{wg} = v^s_{wg}\frac{T}{T^s} \qquad (A-6)$$

and

$$v_{wo} = \frac{M_{ww}}{\rho_w} \qquad (A-7)$$

where v^s_{wg} is the steam molar volume at p and the corresponding saturation temperature T^s, and ρ^s_w is the water density at T and the corresponding saturation pressure p^s. Both are obtained from steam tables.

Equation (A-6) states that the steam molar volume behaves like an ideal gas. Equation (A-7) states that the water-component molar volume in the oil phase is equal to the water-phase molar volume.

The ideal mixing rule calculates phase volume according to

$$v_j = \sum_{i=1}^{N_c-\chi} x_{ij}v_{ij} + x_{wj}v_{wj} \qquad (A-8)$$

where v_{ij} is the volume of component i in phase j. The v_{ij} for the oil phase is given by the correlation

$$v_{io} = \frac{1}{\rho^0_{io}(1-t_{io}(T-T^0)+c_{io}(p-p^0))} \qquad (A-9)$$

The v_{ij} for the gas phase is obtained from the gas component compressibility

$$v_{ig} = \frac{Z_{ig}RT}{p} \qquad (A-10)$$

The gas component compressibility is obtained from tables of gas compressbilities versus pressure and temperature.

Interfacial Tension

The gas-oil interfacial tension is calculated from the Macleod-Sugden correlation[7].

Viscosity

The Lohrenz-Bray-Clark (LBC)[8] correlation or the ideal mixing rule is used for oil and gas viscosity calculations. In addition, the Lee-Gonzales-Eakin (LGE)[9] formula is available for gas viscosity calculations.

The ideal mixing rule calculates the phase viscosities according to

$$\mu_o = \prod_{i=1}^{N_c-\chi} (\mu_{io})^{x_{io}} \times (\mu_{wo})^{x_{wo}} \qquad (A-11)$$

$$\mu_g = \sum_{i=1}^{N_c-\chi} \mu_{ig}x_{ig} + \mu_{wg}x_{wg} \qquad (A-12)$$

The component viscosities, μ_{ij}, are obtained from component viscosity versus temperature tables. The water component viscosity is calculated by

$$\mu_{wo} = \mu_w \qquad (A-13)$$

$$\mu_{wg} = \mu_{s1}T + \mu_{s2} \qquad (A-14)$$

Using the LGE formula, the simulator first calculates μ_{ng}, the gas viscosity of the mixture excluding the water component. The phase viscosity is then obtained by molar averaging as follows:

$$\mu_g = \mu_{ng}x_{ng} + \mu_{wg}x_{wg} \qquad (A-15)$$

Enthalpy and Internal Energy

Like the volume calculation, either the PR3 method or the ideal mixing rule can be used for phase enthalpy. The phase internal energy is assumed to be equal to its enthalpy for the oil phase; that for the gas phase is calculated by

$$u_g = h_g - 0.1852pv_g \qquad (A-16)$$

With the PR3 method, the simulator first calculates h_{nj}, the partial molar enthalpy of the N_c components as follows:

$$h_{nj} = h^o_{nj} + RT(Z_j - 1) + (T\frac{\partial a}{\partial T} - a)\frac{1}{2.828b}\ln(\frac{Z_j + 2.414B}{Z_j - 0.414B}) \qquad (A-17)$$

where the h^o_{nj} is the ideal gas enthalpy.

The h_{nj} is the phase enthalpy, if the N_c components include all the components in that phase. However, if the N_c components does not include water components, which is the case when χ =0, the phase enthalpy is obtained by molarly averaging the partial molar enthalpy of the N_c components and the partial molar enthalpy of the water component as follows:

$$h_j = x_{nj}h_{nj} + (1-\chi)x_{wj}h_{wj} \qquad (A-18)$$

The h_{wj} is calculated as follows:

$$h_{wg} = u_{wg} + 0.1852pv_{wg} \qquad (A-19)$$

$$u_{wg} = u^s_{wg} + C_{pw}(T - T^s) \qquad (A-20)$$

and

$$h_{wo} = u_{wo} = u_w = u^s_w \qquad (A-21)$$

where u^s_{wg} is the steam molar internal energy at p and the corresponding saturation temperature T^s, and u^s_w is the water internal energy at T and the corresponding saturation pressure p^s. Both are obtained from Steam Tables.

Equation (A-21) states that the water component internal energy in the oil phase is equal to the water phase molar internal energy.

The ideal mixing rule calculates phase enthalpy according to

$$h_j = \sum_{i=1}^{N_c-\chi} x_{ij}h_{ij} + x_{wj}h_{wj} \qquad (A-22)$$

where h_{ij} is the enthalpy of component i in phase j. The h_{ij} for the oil phase is given by the correlation

$$h_{io} = C_{pio}(T - T^1) \qquad (A-23)$$

The h_{ij} for the gas phase is given by

$$h_{ig} = C_{pio}(T_{bi} - T^1) + H_{vi} + C_{pig1}(T - T_{bi}) + \frac{C_{pig2}(T^2 - {T_{bi}}^2)}{2} + \frac{C_{pig3}(T^3 - {T_{bi}}^3)}{3} + \frac{C_{pig4}(T^4 - {T_{bi}}^4)}{4} \qquad (A-24)$$

APPENDIX B : DESCRIPTION OF MODEL A

PROBLEM STATEMENT:

Steam displacement of a distillable oil.

GRID:

18x18x4

The areal dimensions of all grids are 29.17 ft x 29.17 ft.

The thicknesses of the four layers are 10 ft, 20 ft, 25 ft, and 25 ft from top to bottom.

The subsea depth to the top layer is 1500 ft.

Two injection wells are located at the northwest and southeast corners and two production wells are located at the northeast and southwest corners.

The injection wells are perforated at the bottom layer and the production wells are perforated at all layers. The completion productivity index for the injection well is 12.632 cp-bbl/day/psia and those for the production well are 5.053, 2.527, 6.316, 12.632 cp-bbl/day/psia from top to bottom.

INITIAL CONDITIONS:

Oil saturation = 55%

Water saturation = 45%

Reservoir temperature = 125 °F

Pressure at the center of the top layer = 75 psia

No capillary pressure

FLUID AND ROCK PROPERTIES:

Same as those in problem No. 3 of the Fourth SPE Comparative Solution Project[4].

OPERATING CONDITIONS:

Inject steam into both injection wells and produce from both production wells for 1 year. The steam quality is 0.7 at 450 °F. Steam is injected subject to a maximum bottom hole pressure of 1000 psia and a maximum rate of 300 STB/day (CWE). Oil is produced at a constant bottom hole pressure of 17 psia.

APPENDIX C : DESCRIPTION OF MODEL C

PROBLEM STATEMENT:

Steam displacement of a light oil.

GRID:

7x1x3

The areal dimensions of all grids are 500.0 ft x 3500.0 ft.

The thicknesses of the three layers are 20 ft, 30 ft, and 50 ft from top to bottom.

The subsea depth to the top layer is 8325 ft.

An injection well is located at the left side of the grid and a production well is located at the right side of the grid.

The injection well is perforated at the top layer and the production well is perforated at the bottom layer. The completion productivity indices for both wells are 66.37 cp-bbl/day/psia.

INITIAL CONDITIONS:

Oil saturation = 80%

Water saturation = 20%

Reservoir temperature = 174 °F

Pressure at the depth of 8400 ft = 4000 psia

FLUID AND ROCK PROPERTIES:

For fluid properties, see Table 5, 6, and 7.

Porosities, permeabilities, and relative permeabilities are the same as those in the Fifth SPE Comparative Solution Project[10].

Rock heat capacities and thermal conductivities are the same as those in problem No. 3 of the Fourth SPE Comparative Solution Project[4].

OPERATING CONDITIONS:

Oil is produced subject to a minimum bottom hole pressure of 1000 psia and a maximum rate of 12000 STB/day. No injection for 1 year. Afterwards, inject steam into the injection well and produce from the prodction well for 3000 days. The steam quality is 0.3 at 300 °F. Steam is injected subject to a maximum bottom hole pressure of 3000 psia and a maximum rate of 45000 STB/day (CWE).

Table 1: Summary of Equations and Unknowns

Equation	Eq. No.	Unknowns
Hydrocarbon Material Balance Equation	(1)	x_{ie} $i = 1, N_c - \chi$
Water Material Balance Equation	(3) or (4)	S_w
Energy Balance Equation	(6)	T
Hydrocarbon Phase Fugacity Equality	(7) or (8)	x_{i2} $i = 1, N_c$
Hydrocarbon-Water Phase Fugacity Equality when $\chi = 1$	(9) or (10) or (11)	x_{wa}
Gas-Water Phase Fugacity Equality when $\chi = 0$	(12)	y_w
Volume Equation	(13)	v_j $j = 1, N_h$
Saturation Constraint	(14)	p
Composition Constraint	(15)	S_j $j = 1, N_h$

Table 2: Selection of Primary Variables

Fluid Type	Boiling Point Range	Primary Variables
Gas-oil-water	Narrow	$p, x_{21}, ..., x_{Nc1}, z_w, S_g$
Gas-oil-water	Wide	$p, x_{21}, ..., x_{Nc1}, z_w, T$
Gas-water	Narrow	$p, x_{22}, ..., x_{Nc2}, z_w, S_g$
Gas-water	Wide	$p, x_{22}, ..., x_{Nc2}, z_w, T$
Gas-oil	.....	$p, S_g, x_{21}, ..., x_{Nc1}, y_w, T$
Oil-water	.....	$p, x_{21}, ..., x_{Nc1}, z_w, T$
Gas	.....	$p, x_{22}, ..., x_{Nc2}, y_w, T$

Table 3: Speedup as a Function of Vector Length

		Vector Length (NVR)			
Calculation	Vector off	10	100	400	1296
PHYSIC	1.0	1.48	6.94	7.46	8.17
FLOW	1.0	1.34	7.08	7.89	9.05
SOURCE	1.0	1.14	1.40	1.22	1.24
OUTPUT	1.0	1.00	1.01	1.01	1.02

Table 4: Speedup of a Vectorized Thermal Simulator (V) over a Conventional Thermal Simulator (C)

	Normalized Speedup	
MODEL	C	V
A	1.0	5.14
B	1.0	5.81

Table 5: Fluid Composition and Equation of State Parameters

Component	x	Mw	$p_c(atm)$	$T_c(K)$	$v_c(l/gmole)$	ω	S_c
Methane	0.5391	16.04	45.80	190.7	0.099	0.013	-0.154
Ethane	0.1252	30.07	48.20	305.43	0.148	0.0986	-0.1002
n-Butane	0.1245	58.12	37.47	425.2	0.255	0.201	0.06413
n-Heptane	0.1138	100.20	27.01	540.16	0.426	0.3498	0.01223
C10+	0.0974	273.00	14.17	815.18	1.1945	0.7883	0.1763
Water	0.0000	18.015	217.6	647.3	0.056	0.344	0.180

Table 6: Parameters for Component Oil Density Calculations

Component	$\rho^0_{10}(lb/cft)$	$c_{10}(1/psia)$	$t_{10}(1/R)$
Methane	16.70	6.53×10^{-6}	5.3×10^{-4}
Ethane	28.30	6.53×10^{-6}	5.3×10^{-4}
n-Butane	36.54	6.53×10^{-6}	5.3×10^{-4}
n-Heptane	42.75	6.53×10^{-6}	5.3×10^{-4}
C10+	52.89	6.53×10^{-6}	5.3×10^{-4}

Table 7: Parameters for Component Enthalpy Calculations

Component	C_{pio} $(Btu/lb - F)$	C_{pig1} $(Cal/gmole - K)$	C_{pig2} $(Cal/gmole - K^2)$	C_{pig3} $(Cal/gmole - K^3)$
Methane	.50	4.598	1.245×10^{-2}	2.86×10^{-6}
Ethane	.50	1.292	4.254×10^{-2}	-1.657×10^{-5}
n-Butane	.50	2.266	7.913×10^{-2}	-2.647×10^{-5}
n-Heptane	.50	−1.229	1.615×10^{-1}	-8.720×10^{-5}
C10+	.50	−3.70	4.329×10^{-1}	-2.424×10^{-4}

Component	C_{pig4} $(Cal/gmole - K^4)$	T_{bi} (K)	H_{vi} $(Cal/gmole)$
Methane	-2.703×10^{-9}	111.7	1955.
Ethane	2.081×10^{-9}	184.5	3515.
n-Butane	-0.674×10^{-9}	272.7	5352.
n-Heptane	1.829×10^{-8}	371.6	7576.
C10+	5.267×10^{-8}	634.0	14014.

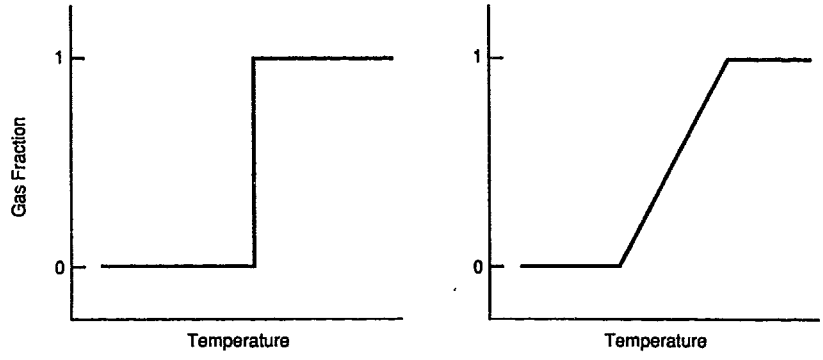

(a) Narrow Boiling Point Range (b) Wide Boiling Point Range

Figure 1

Boiling Point Range in a Constant Pressure Vaporization Process.

Figure 2: Speedup as Function of Vector Length

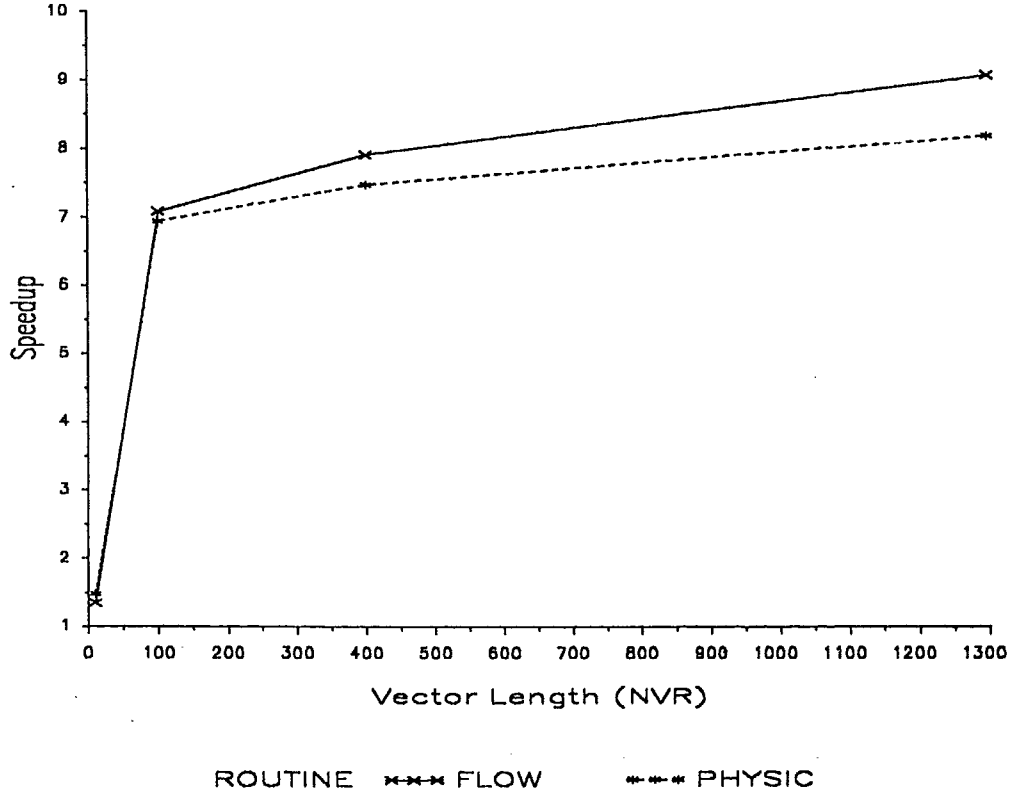

Fig. 3 : AVERAGE PRESSURE
USING DIFFERENT PHYSICAL PROPERTY CALCULATION METHODS
(Light Oil Steam Flood)

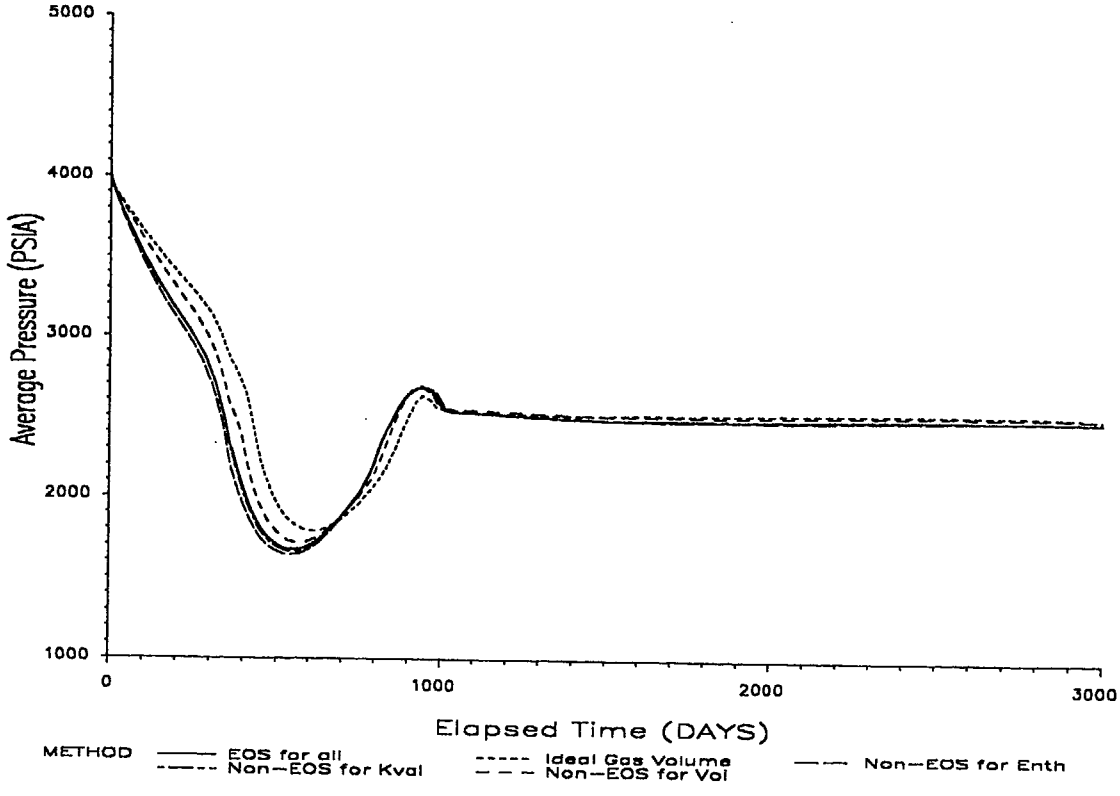

Fig. 4: AVERAGE TEMPERATURE
USING DIFFERENT PHYSICAL PROPERTY CALCULATION METHODS
(Light Oil Steam Flood)

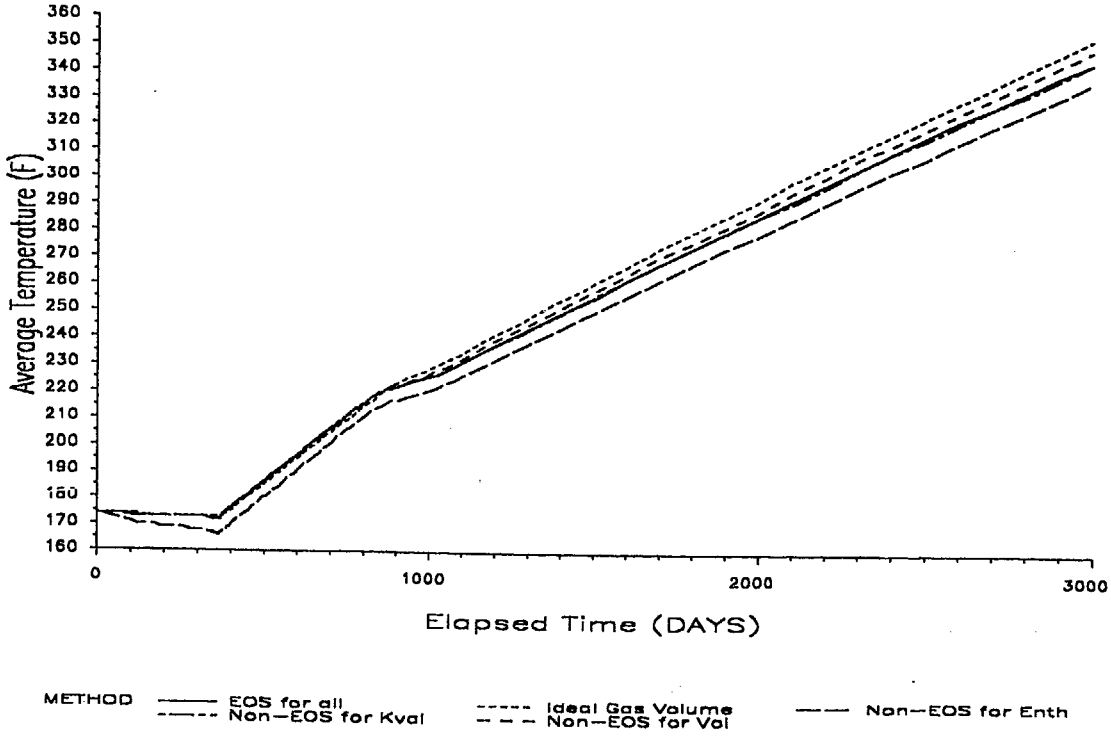

Fig. 5: CUMULATIVE OIL PRODUCED
USING DIFFERENT PHYSICAL PROPERTY CALCULATION METHODS
(Light Oil Steam Flood)

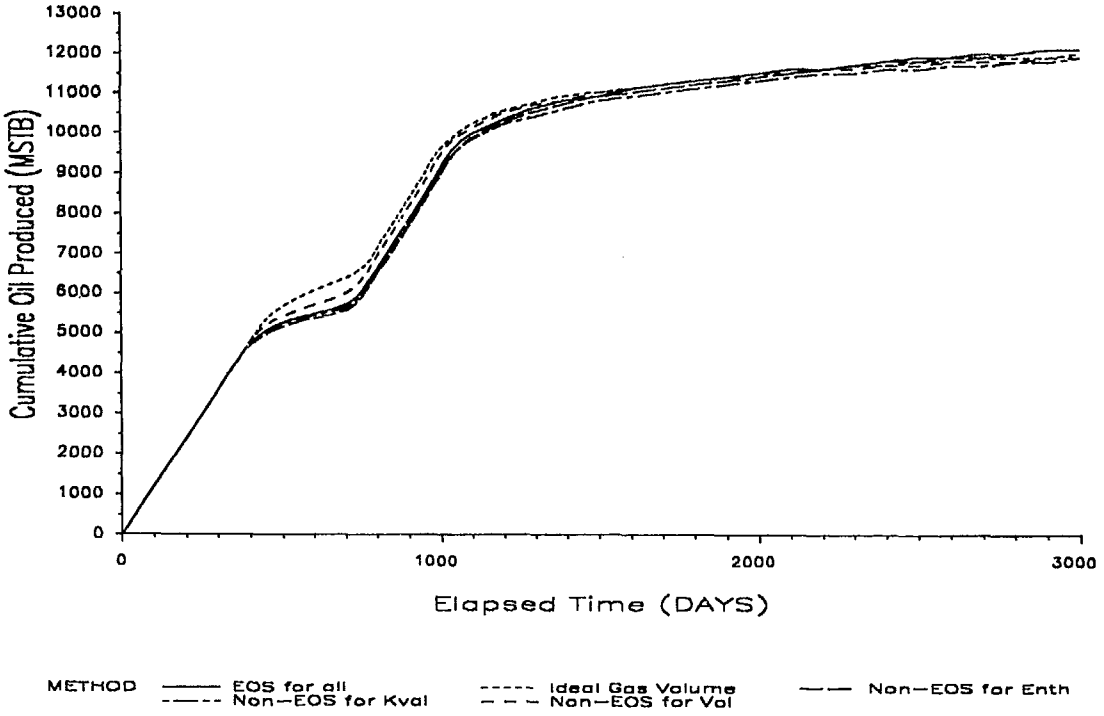

Fig. 6: CUM OIL PRODUCED VS. CUM WATER INJECTED
USING DIFFERENT PHYSICAL PROPERTY CALCULATION METHODS
(Light Oil Steam Flood)

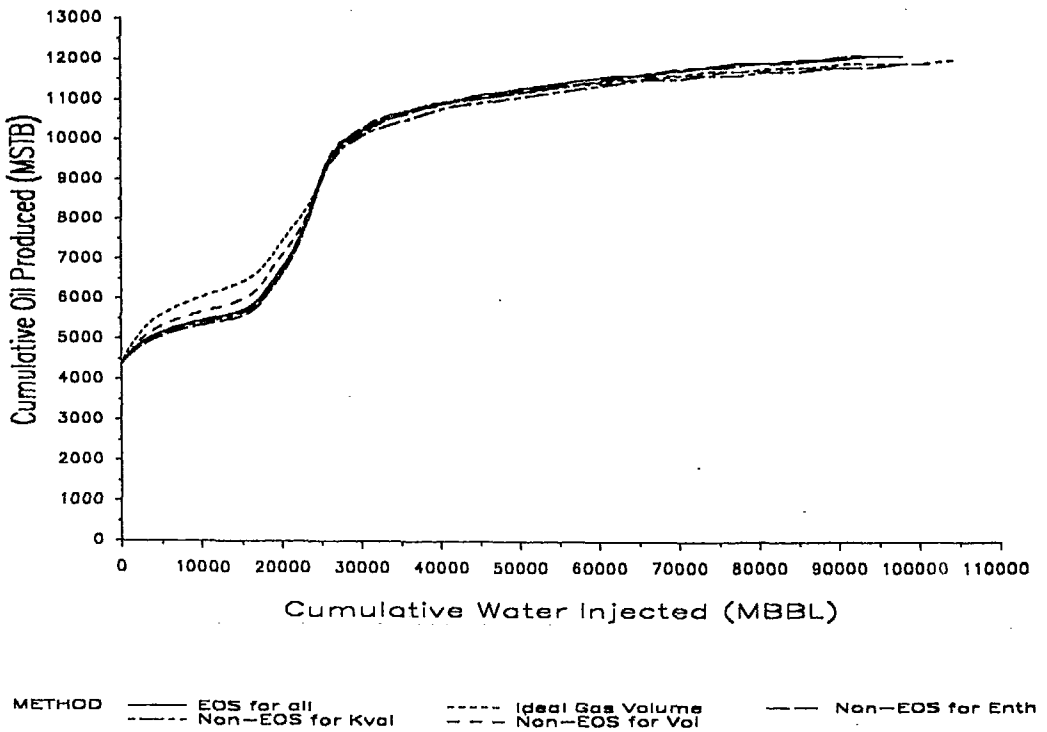

Fig. 7: GOR PRODUCED
USING DIFFERENT PHYSICAL PROPERTY CALCULATION METHODS
(Light Oil Steam Flood)

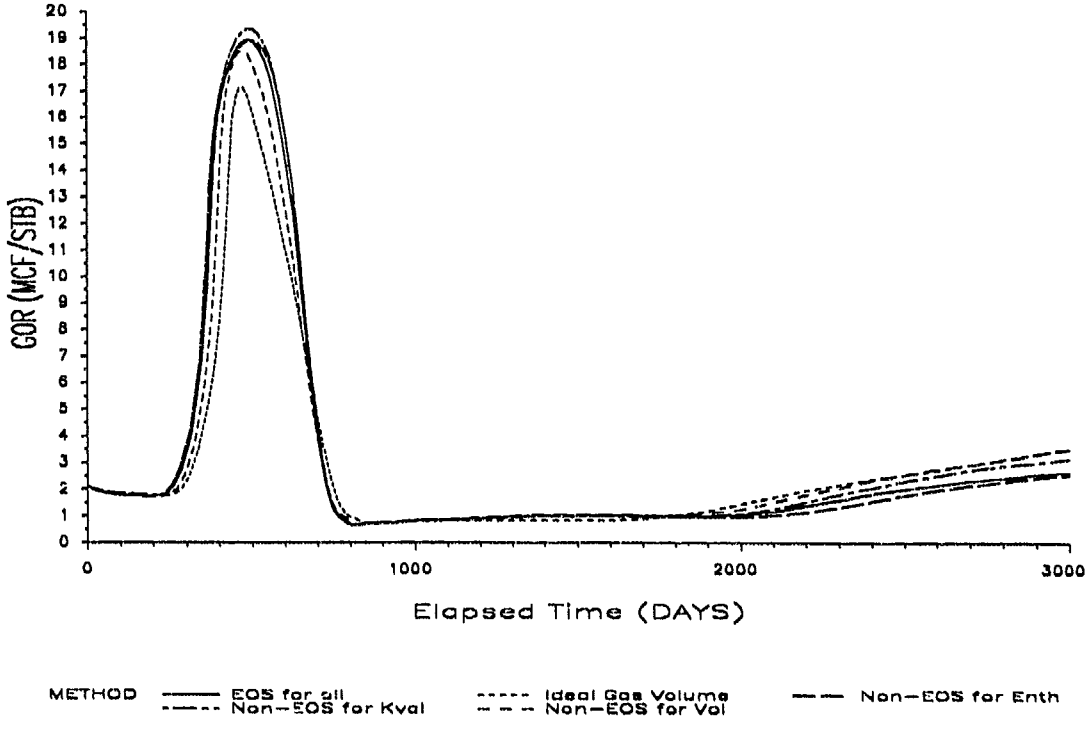

Fig. 8: WOR PRODUCED
USING DIFFERENT PHYSICAL PROPERTY CALCULATION METHODS
(Light Oil Steam Flood)

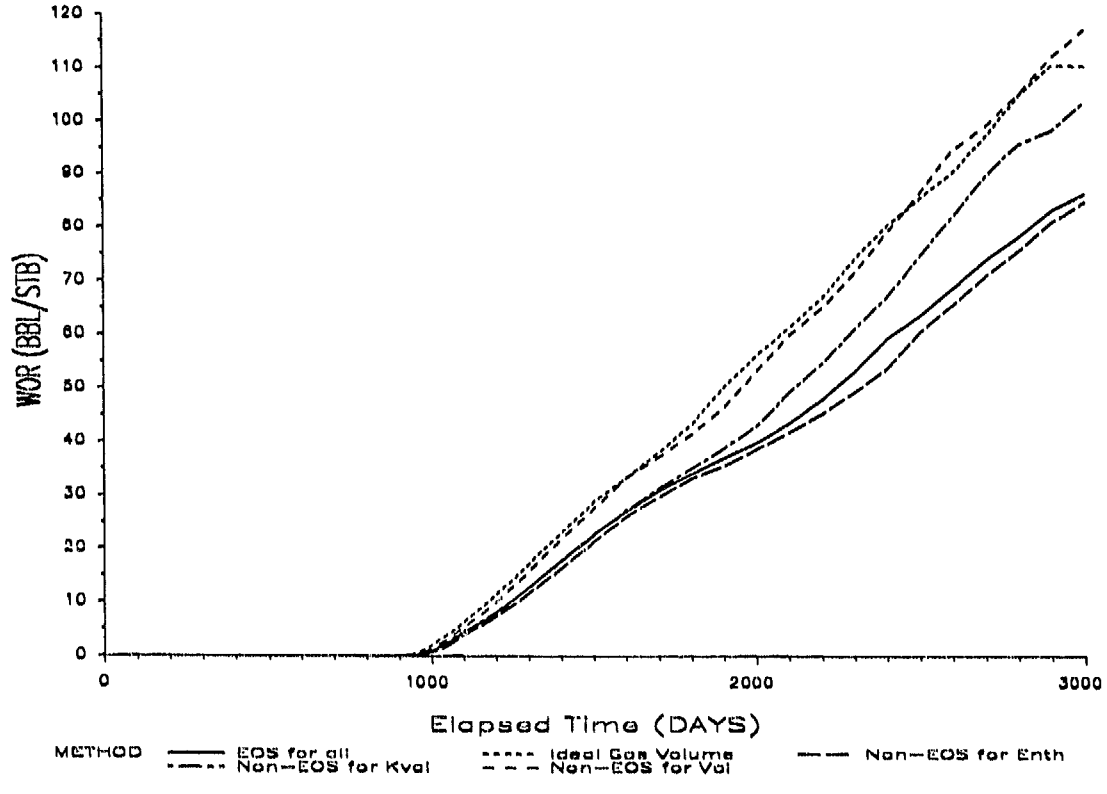

Fig. 9: AVERAGE PRESSURE
USING DIFFERENT PHYSICAL PROPERTY CALCULATION METHODS
(Light Oil Steam Flood)

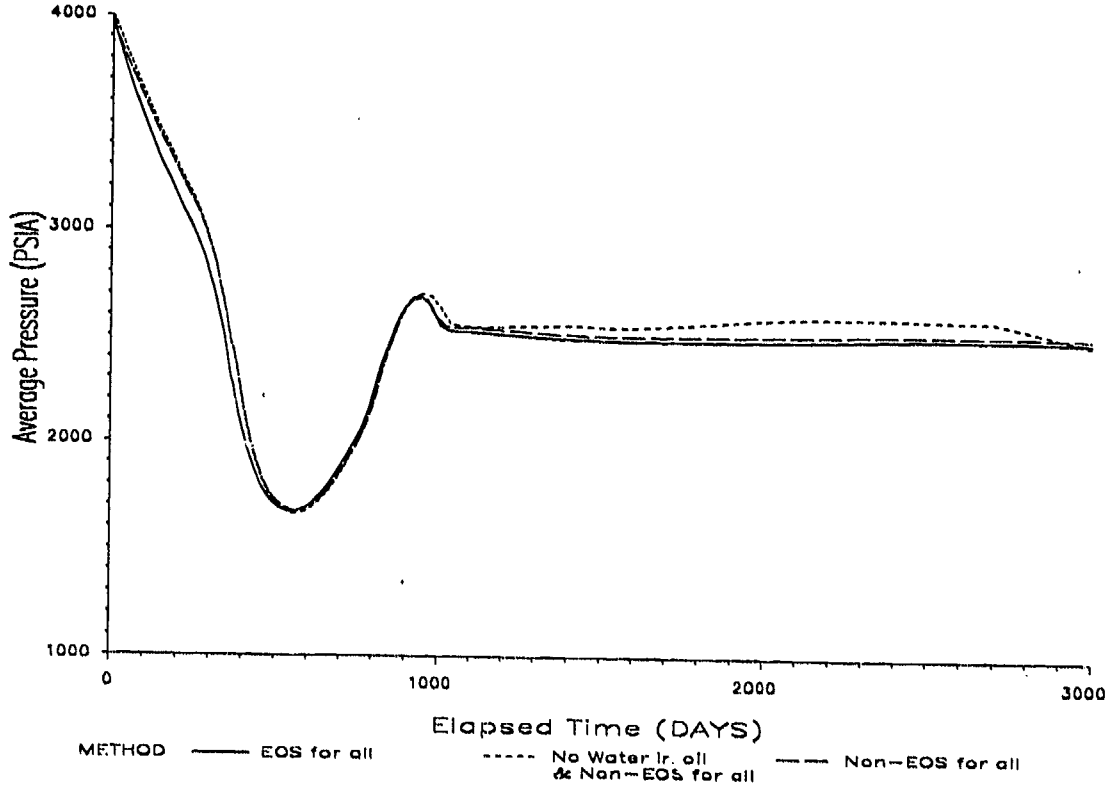

Fig. 10: AVERAGE TEMPERATURE
USING DIFFERENT PHYSICAL PROPERTY CALCULATION METHODS
(Light Oil Steam Flood)

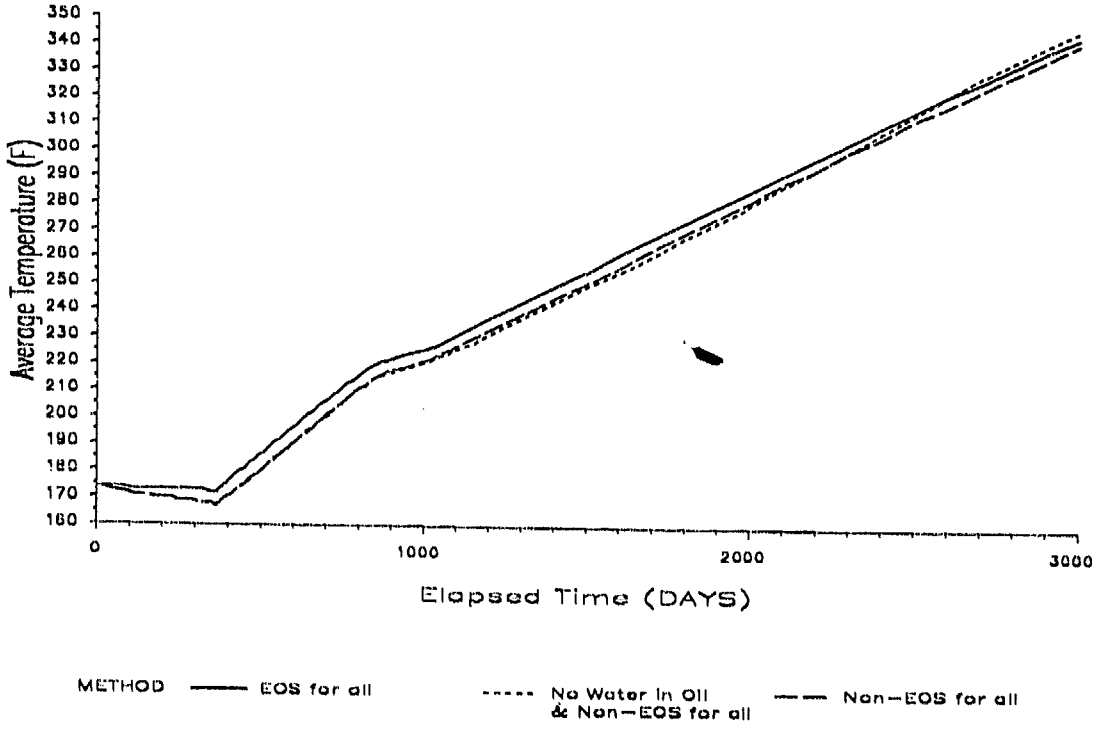

Fig. 11: CUMULATIVE OIL PRODUCED
USING DIFFERENT PHYSICAL PROPERTY CALCULATION METHODS
(Light Oil Steam Flood)

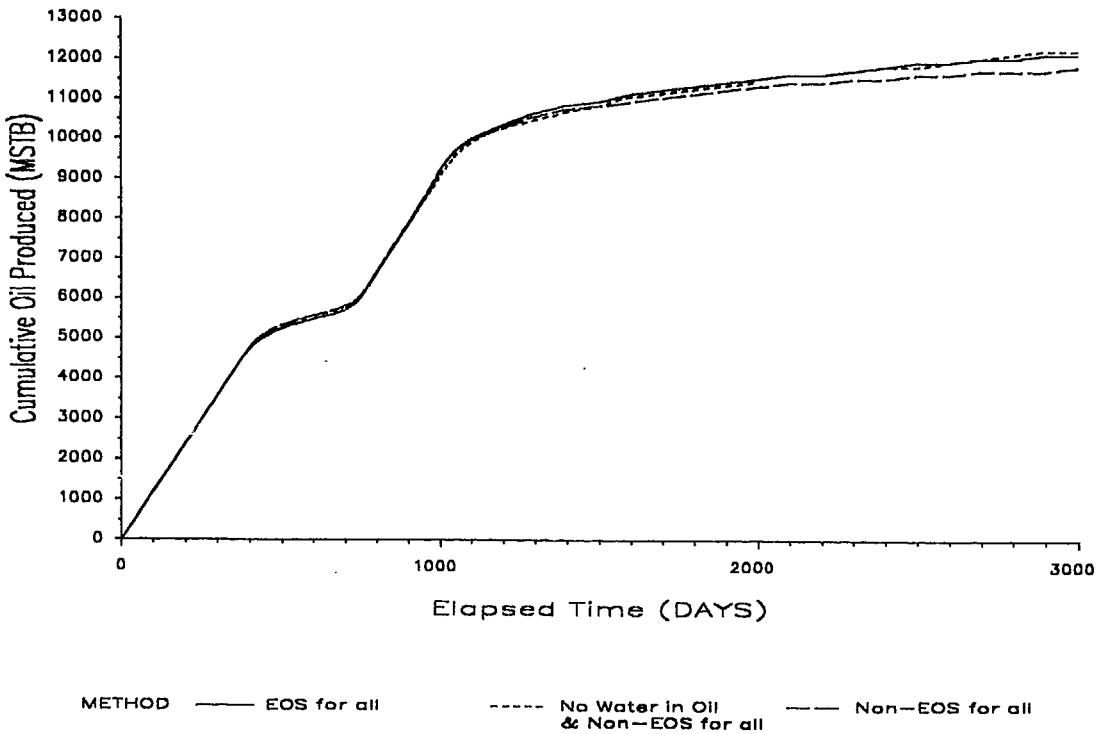

Fig. 12: CUM OIL PRODUCED VS. CUM WATER INJECTED
USING DIFFERENT PHYSICAL PROPERTY CALCULATION METHODS
(Light Oil Steam Flood)

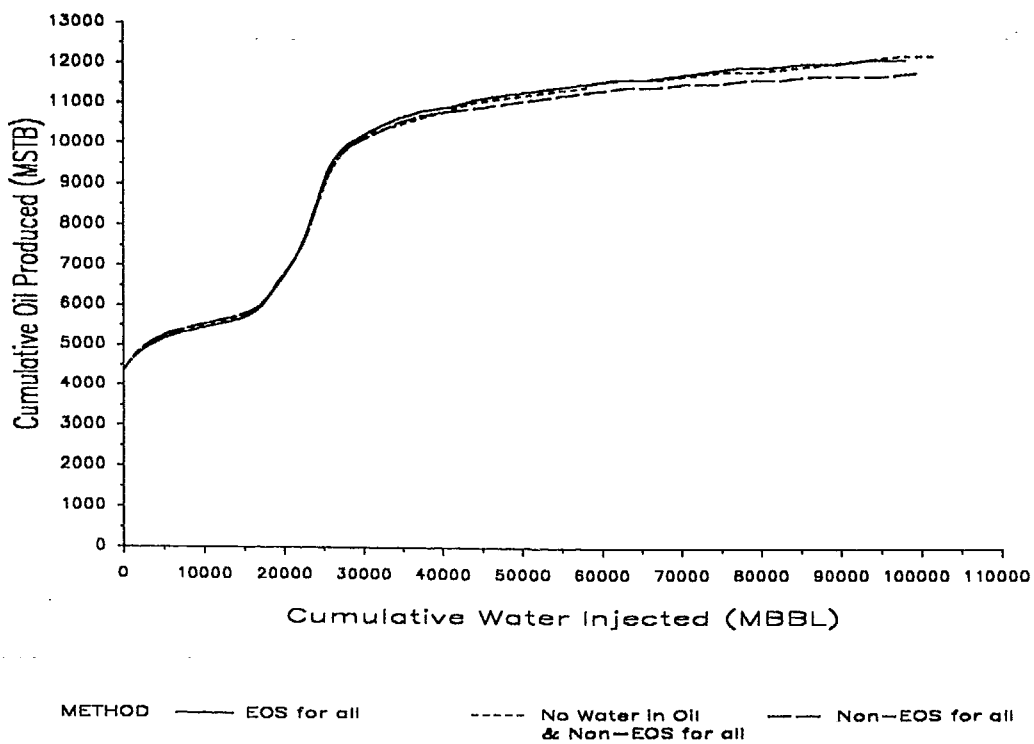

Fig. 13: GOR PRODUCED
USING DIFFERENT PHYSICAL PROPERTY CALCULATION METHODS
(Light Oil Steam Flood)

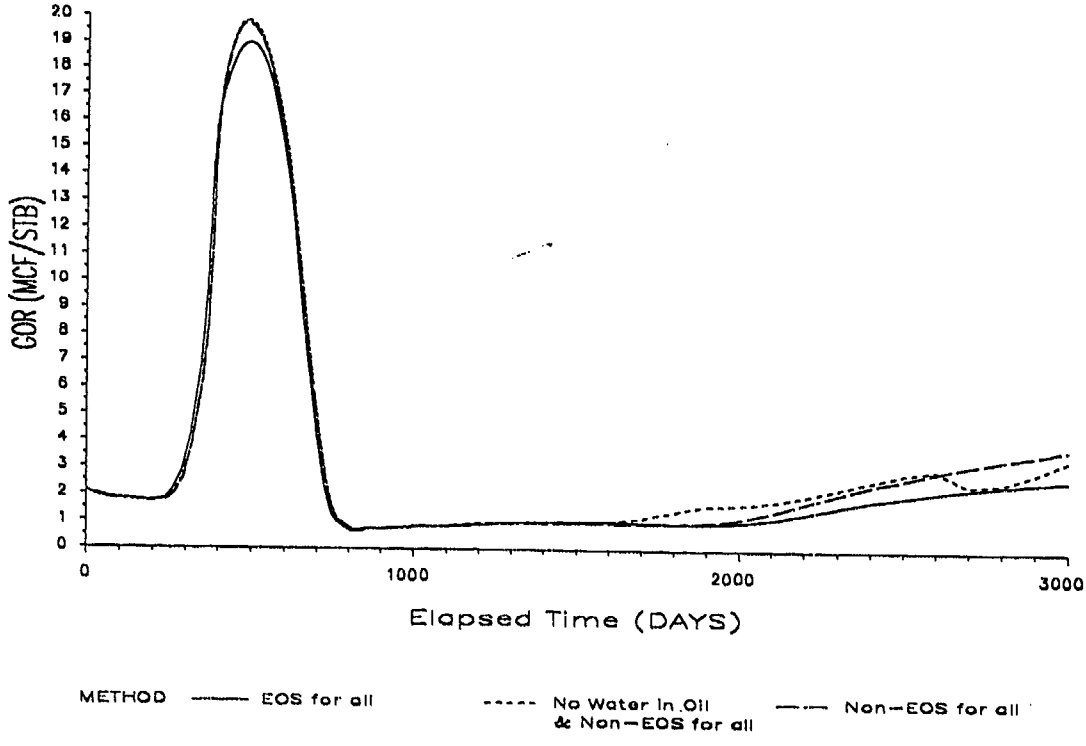

Fig. 14: WOR PRODUCED
USING DIFFERENT PHYSICAL PROPERTY CALCULATION METHODS
(Light Oil Steam Flood)